Macromolecules

NOTE

pubs.acs.org/Macromolecules

Effects of Block Architecture on Structure and Mechanical Properties of Olefin Block Copolymers under Uniaxial Deformation

Feng Zuo, Yimin Mao, Xiaowei Li, Christian Burger, and Benjamin S. Hsiao*

Department of Chemistry, Stony Brook University, Stony Brook, New York 11794, United States

Hongyu Chen and Gary R. Marchand

The Dow Chemical Company, Freeport, Texas 77541, United States

Thermoplastic elastomers have become substitutes for natural and synthetic rubbers in many applications because they can be easily compounded by traditional thermoplastic processing methods. Conventional thermoplastic elastomers include styrenic block copolymers,[1,2] polyurethanes,[3,4] thermoplastic elastomer blends,[5] and polyolefin elastomers and plastomers.[6] The Dow Chemical Company recently introduced a novel class of olefin block copolymers (OBC) made from ethylene and a higher α-olefin using chain shuttling technology.[7−15] Polymer chains in OBCs comprise two or more different blocks, with different comonomer content, connected in a linear manner. The hard block is a random ethylene copolymer segment containing very low α-olefin comonomer content and thus has a relatively high density and a high melting temperature. The soft block is also a random ethylene copolymer segment, containing much higher comonomer content, and thus has a lower density and limited crystallinity. The formation of linearly segmented OBC chains in one reactor is achieved by employing two catalysts with different comonomer selectivity and one chain shuttling agent that can transfer the growing chains between two catalysts reversibly. So, an increase in chain shuttling agent content leads to more frequent transfers of growing chains during polymerization, resulting in shorter and more blocks and thus directly affecting the block architecture in OBCs.

The effects of block architecture on the structure, morphology, and mechanical properties of styrenics, polyurethanes, and other segmental block copolymer systems have been documented in the literature. These effects include soft block length,[16−20] hard block length,[21−24] content of each block,[25−27] and the length and number of blocks.[28,29] In our previous work,[30] we investigated the differences in structural changes and mechanical properties between OBC and ORC (olefin random copolymer). We demonstrated that better connectivity and effective network structure in ORC resulted in a higher degree of orientation. In this work, we compared a previously studied OBC with one more OBC that was synthesized with a higher chain shuttling agent content. The two OBCs have similar molecular weight and the same volume fraction and comonomer content of each block, but different block architecture. *In-situ* synchrotron wide-angle X-ray diffraction (WAXD) and small-angle X-ray scattering (SAXS) combined with tensile testing apparatus were used to simultaneously study the structural change, orientation development, and mechanical properties of the two OBCs during uniaxial and step-cyclic deformation at different temperatures. Finally, a structure model is proposed to explain the relationship between the mechanical properties and block architecture resulting from the different content of the chain shuttling agent used during polymerization.

The two chosen OBCs, OBC-LS (also reported in our previous study[30]) and OBC-HS, were ethylene−octene block copolymers provided by The Dow Chemical Company. The sample information is shown in Table 1. Molecular weight was measured by high-temperature gel permeation chromatography in 1,2,4-trichlorobenzene using polystyrene standards and was converted to polyethylene equivalents. The overall and hard block octene contents were determined by ^{13}C NMR, while the soft block octene content was determined by ^{1}H NMR on material extracted from pellet samples dissolved in *n*-hexane.[12] The block density was estimated according to the octene content. Melting temperature was measured by DSC using a 10 °C/min heating rate, and crystallinity was obtained by comparison to the theoretical heat of fusion of 100% crystalline polyethylene (292 J/g). Both OBCs had nearly the same content of soft block (ca. 80 wt %) with a density of 0.857 g/cm^3, and the remaining 20 wt % hard block had a density of 0.932 g/cm^3. The overall density and weight averaged molecular weight of these two OBCs were very similar to each other. However, OBC-LS was produced with 0.4 chain shuttling agent per 1000 ethylene units, while OBC-HS was produced with 1.3 chain shuttling agent per 1000 ethylene units. Only the hard block in the OBCs could crystallize at room temperature, while the soft block could not.

Engineering stress−strain curves of both OBC-HS and OBC-LS under uniaxial deformation at room temperature, 60 °C, and 90 °C are shown in Figure 1. Stress−strain curves at room temperature exhibit similar features. The Young's moduli for the two OBCs are about the same, ∼9 MPa, which is consistent with the value reported from typical ethylene random copolymers having similar overall density.[31] At the late stage of the deformation (e.g., strain ≥11), strain hardening becomes apparent. Deformation at high temperatures leads to distinct differences between two OBCs. For example, at 60 °C, the fracture strain of OBC-LS reduces significantly, while that of OBC-HS remains relatively high. Another difference is the stress buildup at the early stage, which is faster in OBC-HS than in OBC-LS. The overall trend of the stress−strain curve at 60 °C is quite different

Received: November 4, 2010
Revised: March 7, 2011
Published: April 08, 2011

Table 1. Sample Information of OBCs

	overall density (g/cm^3)	overall octene (mol %)	soft block (wt %)	octene in soft (mol %)	soft block density	octene in hard (mol %)	hard block density	CSA/[C2] × 1000	M_w (kg/mol)	M_w/M_n	T_m (°C)	X_c (wt %)
OBC-LS	0.875	12.1	79	16.7	0.857	0.4	0.932	0.4	124	3.05	120	19
OBC-HS	0.878	11.9	78	16.6	0.857	0.4	0.932	1.3	118	2.23	116	21

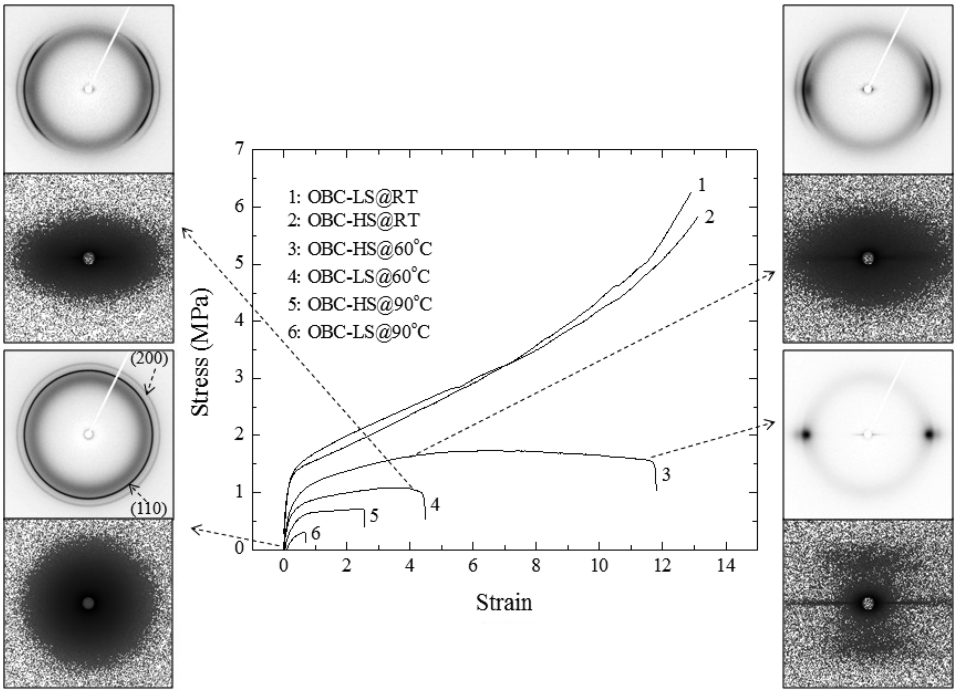

Figure 1. Engineering stress−strain curves of OBC-HS and OBC-LS at room temperature, 60 °C, and 90 °C with selected 2D WAXD and SAXS patterns.

than that at room temperature. At 60 °C, after passing the yield point, the stress reaches a plateau value in both samples and begins to decrease with strain (strain softening) until the sample breaks. This is completely opposite to the strain hardening behavior at room temperature. When OBCs are deformed at an even higher temperature, i.e., 90 °C, a similar trend can be observed.

At 60 °C, selected SAXS and WAXD patterns of OBC-LS at strain 0 and 4, and of OBC-LS at strain 4 and 12, are shown in Figure 1. It is seen that the initial SAXS and WAXD patterns are isotropic, confirming that melt-pressed OBCs have random crystal structure before deformation. Because of the small fracture strain at 60 °C, the polymer chains in OBC-LS can only reach a low degree of crystal orientation before fracture. This is seen in the WAXD pattern of OBC-LS at strain of 4, where the orthorhombic (110) and (200) peaks exhibit very broad spreads, and the corresponding SAXS pattern is elliptical rather than showing a distinct oriented feature. The (010) peak from the monoclinic phase, located between the (110) peak and the amorphous peak, cannot be observed before fracture. In contrast, the WAXD pattern of OBC-HS at a strain of 4 shows the formation of the monoclinic crystal and narrower spreads of (110) and (200) peaks, suggesting a higher crystal orientation and the behavior of strain-induced crystallization. As strain increases to about 12 before fracture, an intense pointlike diffraction pattern, resulting from highly orientated monoclinic

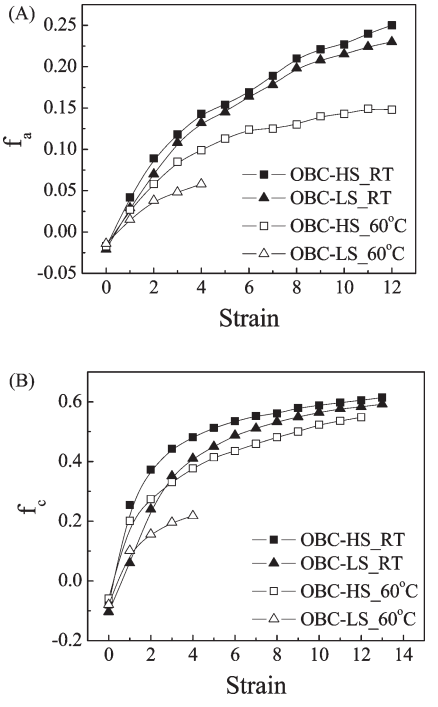

Figure 2. Development of orientation factors of (A) amorphous and (B) orthorhombic crystal phases in OBCs during uniaxial deformation.

dx.doi.org/10.1021/ma102512p |*Macromolecules* 2011, 44, 3670–3673

crystals, is seen on the equator; meanwhile, the corresponding SAXS pattern shows an equatorial streak as well as meridional two-bar scattering peaks.

Hermans' orientation factors (f) for both amorphous and orthorhombic crystal phases were calculated using the method described earlier.[30] The calculated results are shown in Figure 2A, B as a function of strain. The initial f values are slightly negative rather than zero as isotropic samples should be. This is because the equations given for f are for $I(\varphi)$ typically measured by a diffractometer. With a flat plate detector being used here, the azimuthal angle φ is not that between the plane normal and the stretch direction. Instead, a factor of $\cos\theta$ is required for the modification, where θ is the angle that the poles are inclined toward the X-ray source. Since we focused more on comparing the degree of orientation between the two OBCs rather than obtaining the absolute values, the relatively minor correction of $\cos\theta$ was neglected. At room temperature, the orientation factors of both amorphous phases are found to increase to about 0.25 before fracture, which are much lower than that of the crystal phases. It is interesting to note that both orientation factors of crystal and amorphous phases in OBC-HS and OBC-LS are quite close to each other throughout the deformation process at room temperature, although OBC-HS exhibits a slightly higher value. However, the difference between the orientation factors of the two samples becomes quite significant at 60 °C.

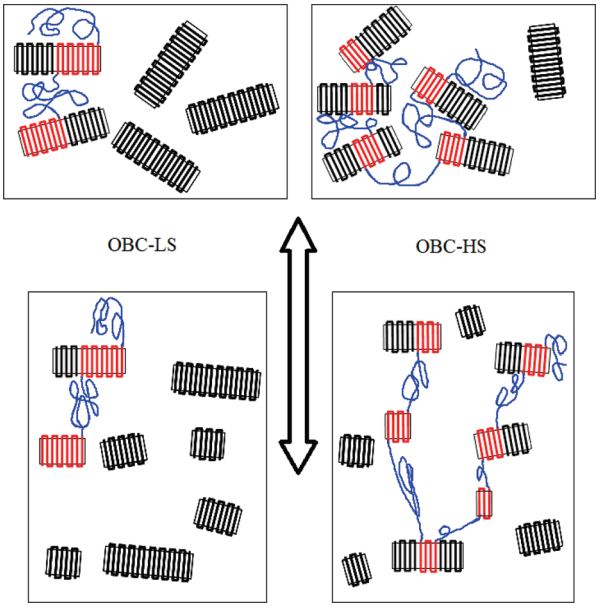

Figure 3. Schematic diagram of the lamellar structure in OBC-LS (left) and OBC-HS (right) before (top) and after (bottom) uniaxial deformation. The entangled amorphous phase is largely neglected except for some tie molecules.

Experimental observations here can be explained from block architecture, resulting from different amounts of chain shuttling agents used during polymerization. Because OBC-LS has longer but fewer hard blocks than OBC-HS, chains in OBC-LS can only be involved in fewer folded-chain lamellar crystals, as illustrated in Figure 3. Consequently, the number of tie chain segments between crystals in OBC-HS is more than OBC-LS. It is known that besides tie chains, chain entanglement can also play a role in affecting tensile properties.[32] However, the entanglement density in both OBCs should be similar because the comonomer content, overall molecular weight, and volume fraction of each block are about the same.[13] Thus, at room temperature, chain disentanglement is difficult as the mobility of amorphous chains is very limited where both tie chains and entanglement points can carry the stress. At high temperatures, the mobility of amorphous chains is greatly enhanced, which would allow the disentanglement process to occur more readily during deformation. This is consistent with the strain-softening behavior observed at high strains. In this case, the role of tie chains becomes dominant. OBC-LS possesses fewer tie chain segments, forming a less effective network structure, and the sample breaks easily at a

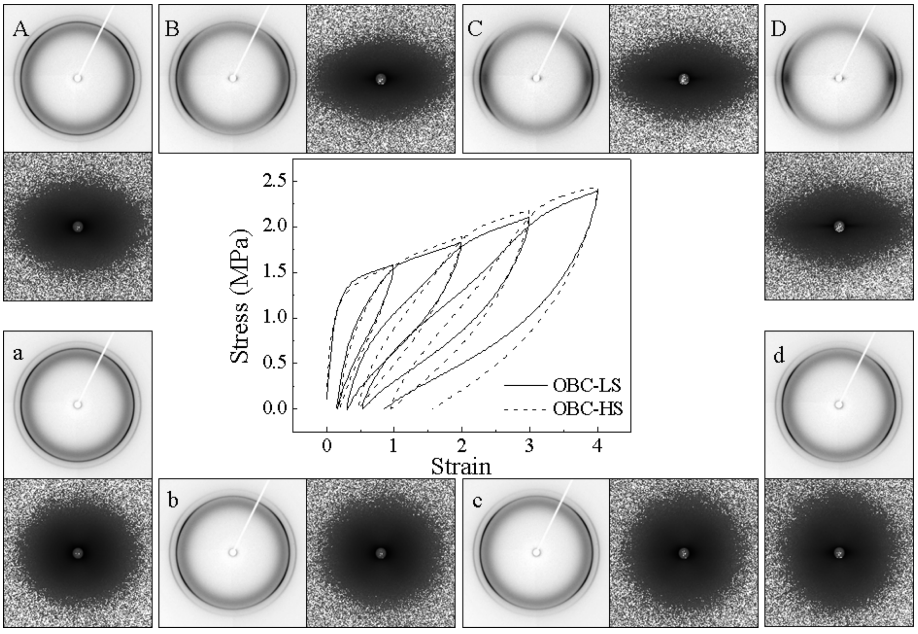

Figure 4. Engineering stress−strain curves and selected 2D SAXS and WAXD patterns of OBC-HS during a step-cyclic test at room temperature. Patterns A, B, C, and D were collected at the stretched states with stains of 1, 2, 3, and 4, while patterns a, b, c, and d were collected after being relaxed to zero stress from A, B, C, and D, respectively.

dx.doi.org/10.1021/ma102512p |*Macromolecules* 2011, 44, 3670–3673

much lower strain at high temperatures. In fact, OBC-HS is more similar to ORC, while OBC-LS is more similar to a polymer blend. Our previous explanation in terms of connectivity and network efficiency also holds up here, since ORC can be viewed as a limited case of the olefin block copolymer having many short soft and hard blocks in one chain.

Step-cyclic tests of OBCs were carried out at room temperature to evaluate the recoverability, and the results are illustrated in Figure 4. From the mechanical behavior, we can conclude that the residual strain of OBC-LS is smaller than that of OBC-HS. This indicates that OBC-LS has better mechanical recoverability than OBC-HS. The 2D SAXS and WAXD patterns also reveal the structural changes upon relaxation. As can be seen when OBC-HS relaxes from 400% strain, the changes between patterns D and d include (1) the relaxation in the degree of orientation and (2) the disappearance of the monoclinic (010) peak. From the point of crystal structure, OBC-HS has a slightly higher crystal fraction and its crystals are more easily stretched and deformed than OBC-LS, thus preventing recovery to the original length upon relaxation. The orientation factors of both amorphous and crystal phases at the stretched state are comparable between the two OBCs. However, when samples are relaxed to zero stress, the difference seems to become larger, especially in the crystal orientation. It is clear that the recovery is a function of the crystalline phase orientation because the higher crystal orientation indicates a better alignment of crystals and also more fragmentation of lamellar crystals. These results again support the proposed molecular mechanism that explains why OBC-LS has a better mechanical recoverability.

AUTHOR INFORMATION

Corresponding Author

*E-mail bhsiao@notes.cc.sunysb.edu; Tel 631-632-7793; Fax 631-632-6518.

ACKNOWLEDGMENT

The authors thank the financial support from the National Science Foundation (DMR-0906512). The assistance of Drs. Lixia Rong and Jie Zhu for synchrotron SAXS and WAXD experimental setup is also greatly appreciated.

REFERENCES

(1) Holden, G.; Kricheldorf, H. R.; Quirk, R. P. *Thermoplastic Elastomers*, 3rd ed.; Hanser/Garden: Cincinnati, OH, 2004.
(2) Holden, G. *J. Elastoplast.* **1970**, *2*, 234–246.
(3) Hepburn, C. *Polyurethane Elastomers*, 2nd ed.; Elsevier Applied Science: London, 1991.
(4) Wirpsza, Z. *Polyurethanes: Chemistry, Technology and Application*; Horwood: New York, 1993.
(5) Abdou-Sabet, S.; Puydak, R. C.; Rader, C. P. *Rubber Chem. Technol.* **1996**, *69*, 476–494.
(6) Batistini, A. *Macromol. Symp.* **1995**, *100*, 137–142.
(7) Arriola, D. J.; Carnahan, E. M.; Hustad, P. D.; Kuhlman, R. L.; Wenzel, T. T. *Science* **2006**, *312*, 714–719.
(8) Wang, H. P.; Khariwala, D. U.; Cheung, W.; Chum, S. P.; Hiltner, A.; Baer, E. *Macromolecules* **2007**, *40*, 2852–2862.
(9) Khariwala, D. U.; Taha, A.; Chum, S. P.; Hiltner, A.; Baer, E. *Polymer* **2008**, *49*, 1365–1375.
(10) Kamdar, A. R.; Wang, H. P.; Khariwala, D. U.; Taha, A.; Hiltner, A.; Baer, E. *J. Polym. Sci., Polym. Phys.* **2009**, *47* (16), 1554–1572.
(11) Hustad, P. D.; Marchand, G. R.; Garcia-Meitin, E. I.; Roberts, P. L.; Weinhold, J. D. *Macromolecules* **2009**, *42*, 3788–2794.
(12) Li, S.; Register, R. A.; Landes, B. G.; Hustad, P. D.; Weinhold, J. D. *Macromolecules* **2010**, *43*, 4761–4770.
(13) Park, H. E.; Dealy, J. M.; Marchand, G. R.; Wang, J.; Li, S.; Register, R. A. *Macromolecules* **2010**, *43*, 6789–6799.
(14) Kuhlman, R. L.; Klosin, J. *Macromolecules* **2010**, *43*, 7903–7904.
(15) INFUSE Olefin Block Copolymers, The Dow Chemical Company, www.dow.com/infuse.
(16) Martin, D. J.; Meijs, G. F.; Renwick, G. M.; McCarthy, S. J.; Gunatillake, P. A. *J. Appl. Polym. Sci.* **1996**, *62*, 1377–1386.
(17) Martin, D. J.; Meijs, G. F.; Gunatillake, P. A.; McCarthy, S. J.; Renwick, G. M. *J. Appl. Polym. Sci.* **1997**, *64*, 803–817.
(18) Gisselfalt, K.; Helgee, B. *Macromol. Mater. Eng.* **2003**, *288*, 265–271.
(19) Chu, B.; Gao, T.; Li, Y.; Wang, J.; Desper, C. R.; Byrne, C. A. *Macromolecules* **1992**, *25*, 5724–5729.
(20) Kong, X.; Tan, S.; Yang, X.; Li, G.; Zhou, E.; Ma, D. *J. Polym. Sci., Part B: Polym. Phys.* **2000**, *38*, 3230–3238.
(21) Miller, J. A.; Lin, S. B.; Hwang, K. K. S.; Wu, K. S.; Gibson, P. E.; Cooper, S. L. *Macromolecules* **1985**, *18*, 32–44.
(22) Versteegen, R. M.; Kleppinger, R.; Sijbesma, R. P.; Meijer, E. W. *Macromolecules* **2006**, *39*, 772–783.
(23) Amitay-Sadovsky, E.; Komvopoulos, K.; Ward, R.; Somorjai, G. A. *Appl. Phys. Lett.* **2003**, *83*, 3066–3068.
(24) Chen, S.; Hu, J.; Liu, Y.; Liem, H.; Zhu, Y.; Liu, Y. *J. Polym. Sci., Part B: Polym. Phys.* **2007**, *45*, 444–454.
(25) Kim, B. K.; Shin, Y. J.; Cho, S. M.; Jeong, H. M. *J. Polym. Sci., Part B: Polym. Phys.* **2000**, *38*, 2652–2657.
(26) O'sickey, M. J.; Lawrey, B. D.; Wilkes, G. L. *J. Appl. Polym. Sci.* **2002**, *84*, 229–243.
(27) Puskas, J. E.; Antony, P.; Fray, M. E.; Altstadt, V. *Eur. Polym. J.* **2003**, *39*, 2041–2049.
(28) Koo, C. M.; Wu, L.; Lim, L. S.; Mahanthappa, M. K.; Hillmyer, M. A.; Bates, F. S. *Macromolecules* **2005**, *38*, 6090–6098.
(29) Koo, C. M.; Hillmyer, M. A.; Bates, F. S. *Macromolecules* **2006**, *39*, 667–677.
(30) Zuo, F.; Burger, C.; Chen, X. M.; Mao, Y. M.; Hsiao, B. S.; Chen, H.; Marchand, G R.; Lai, S.; Chiu, D. *Macromolecules* **2010**, *43*, 1922–1929.
(31) Chum, P. S.; Swogger, K. W. *Prog. Polym. Sci.* **2008**, *33*, 797–819.
(32) Zuo, F.; Keum, J. K.; Chen, X.; Hsiao, B. S.; Chen, H.; Lai, S. Y.; Wevers, R.; Li, J. *Polymer* **2007**, *48*, 6867–6880.